C_{60} Cluster as an Electron Shuttle in a Ru(II)-Polypyridyl Sensitizer-Based Photochemical Solar Cell

Prashant V. Kamat,*[†,‡,§] Mehul Haria,[†] and Surat Hotchandani[||]

Radiation Laboratory and Department of Chemical & Biomolecular Engineering, University of Notre Dame, Notre Dame, Indiana 46556-0579, and Groupe de Recherche en Énergie et Information Biomoléculaires, Université du Québec à Trois-Rivières, Trois Rivières, Québec, Canada G9A 5H7

Received: January 22, 2004; In Final Form: February 28, 2004

The interaction between the excited sensitizer and the redox couple in a photochemical solar cell is an important factor that can decrease the photon-conversion efficiency. We have now employed C_{60} clusters to separate the $Ru(bpy)_2(dcbpy)^{2+}$ (Ru(II) complex) and I_3^-/I^- couple to minimize the sensitizer−redox couple interactions. The C_{60}-modified electrodes (viz., OTE/SnO_2/Ru(II)/C_{60} and OTE/TiO_2/Ru(II)/C_{60}) delivered photocurrent with greater efficiency than did the SnO_2 and TiO_2 films modified with only a Ru(II) dye (viz., OTE/SnO_2/Ru(II) and OTE/TiO_2/Ru(II)). The luminescence quenching of Ru(II)* by I_3^-, which occurs with a rate constant of 1.9×10^{10} M^{-1} s^{-1}, is suppressed following the deposition of a layer of C_{60} clusters. This paper presents a novel concept of employing a redox-active molecular assembly as an electron relay that greatly minimizes the interaction with the excited dye while maintaining the effectiveness of the regeneration cycle.

Introduction

Many research groups around the world are actively involved in improving the efficiency of dye sensitization-based photochemical solar cells. (See, for example, refs 1−4.) Although such cells produce impressive power-conversion efficiency in the range of 10%, efforts continue to improve their performance further. The redox couple that is found to be the most effective for the regeneration of the sensitizer is the I^-/I_3^- couple. The iodide ions donate electrons to the oxidized sensitizer, thereby minimizing the loss of electrons in charge recombination.[5−7] A high concentration of iodide is necessary to regenerate the sensitizer as it reduces the Ru(III) with a rate constant of 1×10^{10} M^{-1} s^{-1}. Although most of the charge injection from the excited sensitizer into the semiconductor is completed on the subpicosecond-to-nanosecond time scale,[8−10] the presence of high concentrations of I^- and I_3^- increases the probability of their interaction with the excited state of the sensitizer. Usually such an energy loss due to the quenching of the excited sensitizer by the redox couple is thought to be small, although recent studies have demonstrated a reductive quenching phenomenon.[11,12] In our earlier study, we estimated the bimolecular quenching rate constant between excited Ru(II) and I^- to be 1×10^8 s^{-1}.[13] However, to the best of our knowledge, the interaction between excited Ru(II) and I_3^- has not yet been probed in detail.

Ways to minimize the excited-state interaction with the redox couple are important if we are interested in maximizing the photoconversion efficiency. In this preliminary communication, we report a novel concept of using C_{60} clusters as an electron shuttle that effectively regenerates the sensitizer but at the same time minimizes direct interaction between the excited sensitizer and redox couple. The principle of this approach is illustrated in Scheme 1.

SCHEME 1: Using an Electron Mediator to Shuttle Electrons for Sensitizer Regeneration

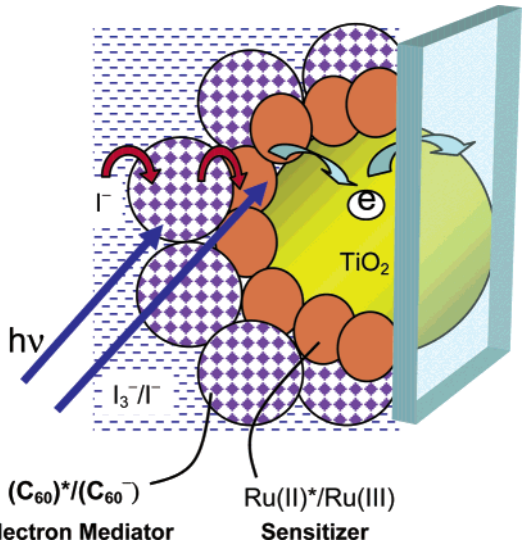

Experimental Section

Materials and Methods. The materials used were of the purest quality available and were used as received. Absorption spectra were recorded using a Shimadzu 3100PC spectrophotometer. Emission lifetime measurements were performed using a laser strobe fluorescence lifetime spectrometer (Photon Technique International). The excitation source was a pulsed N_2 laser (337 nm).

SnO_2 Electrodes. The SnO_2 (15%) suspension obtained from Alfa chemicals was first diluted (1 mL of SnO_2 solution with 47 mL of water and 2 mL of ammonium hydroxide) to obtain a 0.3% solution. This diluted suspension (500 μL) was spread

* Corresponding author. E-mail: pkamat@nd.edu. http://www.nd.edu/~pkamat.
[†] Radiation Laboratory.
[‡] Department of Chemical & Biomolecular Engineering.
[§] Co-op student from McMaster University, Hamilton, Ontario, Canada.
[||] Université du Québec à Trois-Rivières.

10.1021/jp0496699 CCC: $27.50
Published on Web 04/02/2004

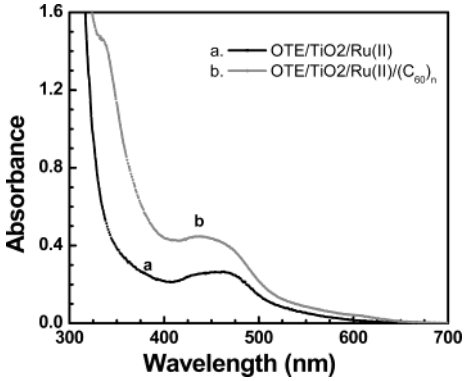

Figure 1. Absorption spectra of OTE/TiO_2/Ru(II) electrodes (a) before and (b) after the deposition of C_{60} clusters.

over a 2-cm^2 area of an optically transparent electrode (OTE). These electrodes were then air dried on a warm plate and annealed in an oven at 673 K for 1 h. Details of the preparation of electrodes can be found elsewhere.[14]

TiO_2 Electrodes. The TiO_2 colloids were formed by the hydrolysis of titanium (IV) hydroxide in acetic acid media. The suspension (500 μL) was spread over the OTE plate using a syringe. After air drying, the electrodes were annealed in an oven at 673 K for 1 h.[15]

SiO_2 Electrodes. The SiO_2 deposition on the OTE was made in the same way as that of SnO_2. A dilute SiO_2 solution (1 mL of SiO_2 (20% stock solution obtained from NALCO), 2 mL of NH_4OH, and 47 mL of water) was made. This suspension (500 μL) was then coated onto the conductive surface of the OTE in two steps. The electrodes were then dried in air and annealed in an oven at 673 K for 1 h.

Ru(II) Complex-Modified Electrodes. A 60 μM solution of Ru(2,2′-bipyridine)$_2$(2,2′-bipyridine-4,4′-dicarboxylic acid)$^{2+}$ (referred to in this paper as Ru(II)) in acetonitrile was transferred to an electrophoretic cell. The optically transparent electrode (OTE) coated with oxide particles and a blank OTE were immersed in this solution with a separating distance of 6 mm. Under the influence of a 100-V dc field, all of the Ru(II) complex was driven to the negative electrode. These electrodes are referred to as OTE/(oxide)/Ru(II). This method enabled us to deposit controlled amounts of Ru(II) onto nanostructured films.

Deposition of C_{60} Clusters. The procedure was similar to the one described earlier.[16,17] C_{60} clusters were prepared by injecting C_{60} solution in toluene (1 mM) into acetonitrile such that the final solvent ratio of toluene/acetonitrile was 10:90. These clusters were then electrophoretically deposited onto the electrodes modified with the oxide and Ru(II) complex. These electrodes are referred to as OTE/(oxide)/Ru(II)/$(C_{60})_n$. C_{60} clusters were also deposited onto blank OTE electrodes without subjecting them to an oxide semiconductor film or Ru(II)-complex modification procedures.

Photoelectrochemical Measurements. Photoelectrochemical measurements were performed using a standard two-compartment cell consisting of a working electrode and a Pt wire gauze counterelectrode. All photoelectrochemical measurements were carried out in acetonitrile containing 0.5 M LiI and 0.01 M I_2. Photocurrents were measured using a Keithley model 617 programmable electrometer. A collimated light beam from a 150-W xenon lamp with a 370-nm cutoff filter was used for the excitation of the electrodes. A Bausch and Lomb high-intensity grating monochromator was introduced into the path of the excitation beam to select an appropriate wavelength. The incident photon-to-photocurrent efficiency (IPCE) at various excitation wavelengths was determined from expression 1.

$$\mathrm{IPCE}(\%) = \frac{i_{sc}}{I_{inc}} \frac{1240}{\lambda} \times 100 \qquad (1)$$

where i_{sc} is the short-circuit photocurrent (A/cm^2), I_{inc} is the incident light intensity (W/cm^2), and λ is the excitation wavelength.

Results and Discussion

The absorption spectra of electrodes OTE/TiO_2/Ru(II) before and after the deposition of C_{60} are shown in Figure 1. The visible absorption is mainly dominated by the Ru(II) complex. C_{60} clusters also show a broad absorbance, more so at wavelengths below 500 nm. Because C_{60} is insoluble in acetonitrile, the electrodes remain undisturbed over long exposure to acetonitrile.

We probed the morphology of these two electrodes using atomic force microscopy (AFM). The tapping-mode AFM images before and after the deposition of C_{60} clusters on OTE/TiO_2/Ru(II) are shown in Figure 2. The Ru(II)-deposited OTE/TiO_2 electrodes essentially show the morphology of the TiO_2 film consisting of an assembly of ~30-nm-diameter particles. The C_{60} clusters deposited onto OTE/TiO_2/Ru(II) electrodes show larger clusters. The deposition of larger-diameter C_{60}

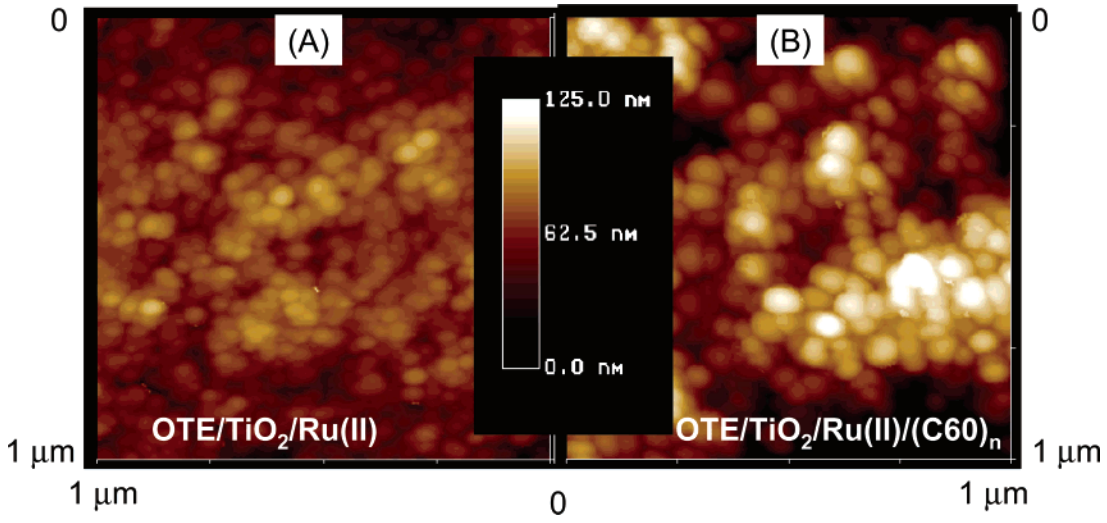

Figure 2. AFM images of OTE/TiO_2/Ru(II) electrodes (A) before and (B) after the deposition of C_{60} clusters.

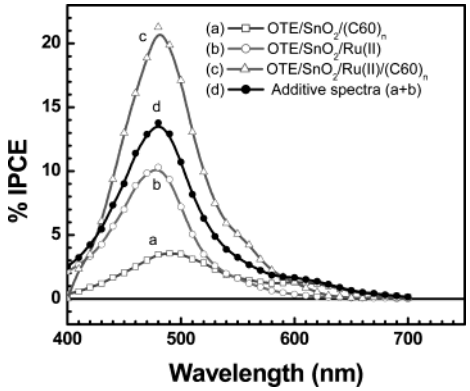

Figure 3. Incident photon to charge carrier generation efficiency (IPCE) of modified nanostructured SnO_2 electrodes immersed in acetonitrile containing I^- and I_3^- electrolytes.

clusters (referred as $(C_{60})_n$) on OTE electrodes and their morphology and electrochemical activity have been discussed in our earlier studies.[17] The C_{60} clusters pack well on the Ru(II)-modified TiO_2 film with a few indiscriminate porous channels. The close packing of these clusters is expected to minimize the interaction between the excited Ru(II)* and I_3^-/I^- redox couple.

Comparison of Photocurrent Generation Efficiencies. The effect of C_{60} cluster deposition on the photoelectrochemical performance has been explored using Ru(II)-modified nanostructured SnO_2 and TiO_2 films. The experiments were carried out in a two-arm flat cell, and the illumination area was limited to 1 cm^2. Figure 3 shows the incident photon to charge carrier generation efficiency (IPCE) of SnO_2 electrodes modified with the Ru(II) complex with and without the presence of a C_{60} layer. The C_{60} cluster deposition on the Ru(II)-modified SnO_2 electrode (viz., OTE/SnO_2/Ru(II)/$(C_{60})_n$ shows an IPCE (spectrum c) that is nearly 2 times higher than that of the Ru(II)-modified SnO_2 electrode (spectrum b). The blank C_{60} cluster-modified SnO_2 electrode shows photocurrent response in the visible with a maximum IPCE around 3% (curve a).

In our earlier study, we presented a photogalvanic mechanism of photocurrent generation at a C_{60} cluster-modified SnO_2 electrode.[16] The excited C_{60} clusters interact with I^- to produce C_{60} anions in the cluster (reaction 2).

$$(C_{60})_n^* + I^- \rightarrow (C_{60})_n^- + I^\bullet \qquad (2)$$

The C_{60} anions formed in the clusters are relatively long-lived[18] and deliver charge to the collecting electrode surface, thereby producing an anodic photocurrent. Photocurrent generation using C_{60} clusters and the iodide couple was presented earlier.[16] The maximum IPCE observed for the C_{60} electrode alone is usually low (less than 5%). Whereas the formation of C_{60} anions producing photocurrent as well as the charge injection process can cooperatively contribute to photocurrent generation, the combined effect is smaller than the enhanced IPCE observed with the OTE/SnO_2/Ru(II)/$(C_{60})_n$ electrode. The maximum IPCE obtained from spectrum d, which is an additive spectrum of a and b (Figure 3), is only marginally higher than that of the OTE/SnO_2/Ru(II) electrode. These results point out that the observed enhancement arises from the indirect participation of the C_{60} cluster/C_{60} anion.

We further investigated the beneficial role of C_{60} clusters by depositing them onto a Ru(II)-modified TiO_2 electrode. The comparison of the IPCE spectra that were recorded using TiO_2 electrodes at different modification stages is shown in Figure 4. The OTE/TiO_2/Ru(II)/$(C_{60})_n$ electrode shows a maximum

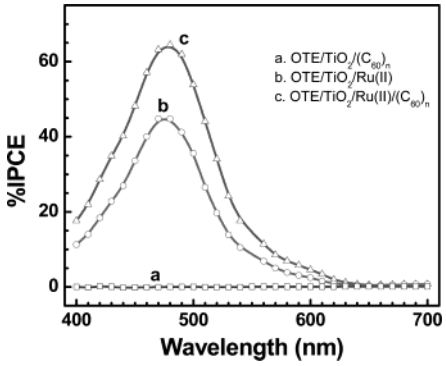

Figure 4. Incident photon to charge carrier generation efficiency (IPCE) of nanostructured TiO_2 electrodes immersed in electrolytes of I^- and I_3^- in acetonitrile.

IPCE of 65% as compared to 50% for the OTE/TiO_2/Ru(II) electrode under similar experimental conditions. The observed higher efficiency for the C_{60}-modified OTE/TiO_2/Ru(II) electrode confirms the beneficial role of C_{60} in mediating the charge-transfer process. Although the observed increase is only ~15%, it is clearly a positive step toward maximizing the photoelectrochemical performance of dye-sensitized solar cells.

Photogenerated C_{60}^- (reaction 1) is electroactive and is long-lived (>100 μs) when generated in clusters and films.[18] It is capable of delivering charge to oxides such as SnO_2.[16] Because the reduction potential of C_{60} is −0.2 V versus NHE, we expect favorable electron transfer to SnO_2 (E_{CB} = 0 V vs NHE) but not to TiO_2 (E_{CB} = −0.5 V vs NHE). This argument is supported by the observed photocurrent response of C_{60}-modified SnO_2 (spectrum a in Figure 3) and TiO_2 (spectrum a in Figure 4). The absence of photocurrent for the OTE/TiO_2/C_{60} electrode shows that C_{60}^- ions cannot directly transfer electrons to TiO_2. Therefore, we can rule out a direct contribution of C_{60}^- to the photocurrent enhancement seen for the OTE/TiO_2/Ru(II)/C_{60} electrode. In a normal photochemical solar cell, iodide ions intercept the oxidized sensitizer (Ru(III)) and facilitate quick regeneration (reaction 3).

$$3I^- + 2Ru(III) \rightarrow I_3^- + 2Ru(II) \qquad (3)$$

The results presented in Figures 3 and 4 further point to the alternate pathway of using C_{60} anions as electron donors to adjacent Ru(III) species formed at the TiO_2 interface (reaction 4).

$$(C_{60})_n^- + Ru(III) \rightarrow (C_{60})_n + Ru(II) \qquad (4)$$

Thus, the C_{60} layer shields most of the Ru(II)* from the triiodide couple while at the same time acting as an electron mediator to regenerate the sensitizer.

If indeed the argument is correct that the quenching of Ru(II)* by I_3^- is minimized by the shielding effect of the C_{60} layer, then we should be able to probe this phenomenon by monitoring the luminescence decay of Ru(II)*. We measured the decay rate constant of Ru(II)* on nanostructured silica film. The silica films were deposited in the same manner as the SnO_2 or TiO_2 films. Silica, being an insulator, does not interact with the excited Ru(II). This allowed us to probe the quenching process of Ru(II)* by I_3^-. A solution of I_3^- was prepared by mixing equal concentrations of I_2 and LiI solution in acetonitrile. An acetonitrile solution of a known concentration of I_3^- was transferred to a square cuvette containing an OTE/SiO_2/Ru(II) electrode. The electrode configuration was such that the back side of the electrode was pressed against the cuvette and excited

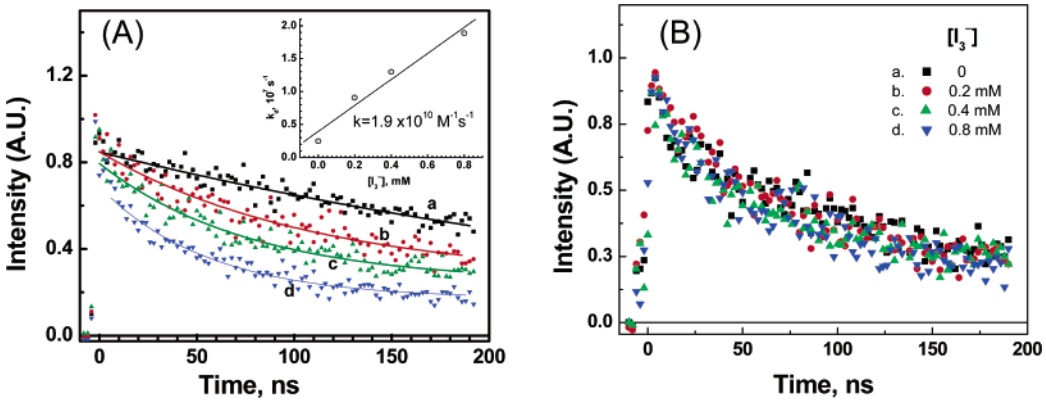

Figure 5. Emission decay traces of (A) OTE/SiO_2/Ru(II) and (B) (A) OTE/SiO_2/Ru(II)/$(C_{60})_n$ electrodes at different concentrations of I_3^-: (a) 0, (b) 0.2, (c) 0.4, and (d) 0.8 mM. Excitation was at 337 nm, and emission was monitored at 600 nm.

SCHEME 2: Excitation and Monitoring Configuration of (a) OTE/SiO_2/Ru(II) and (b) OTE/Ru(II)/(C_{60}) Electrodes[a]

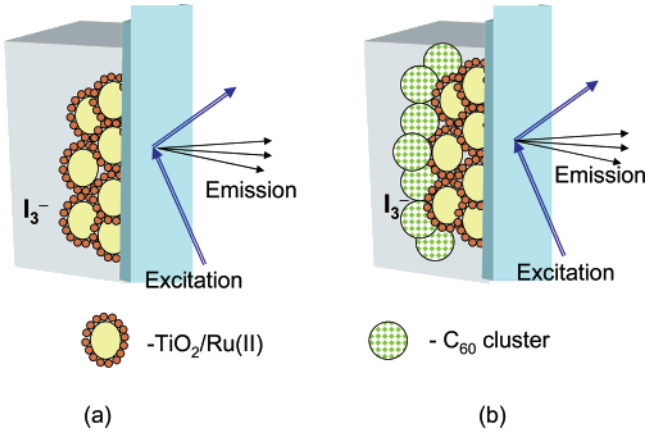

[a] The electrodes were immersed in acetonitrile containing a known amount of I_3^-.

with a 337-nm laser pulse (Scheme 2). The back-side excitation of the electrode minimized the filtering of the excitation pulse by the I_3^- present in the solution. It should be noted that the configuration illustrated in Scheme 2 is an important experimental aspect of these emission measurements.

The emission (600 nm) decay traces were collected in front-face geometry. Parts A and B of Figure 5 show the emission decay at 600 nm of OTE/SiO_2/Ru(II) and OTE/SiO_2/Ru(II)/$(C_{60})_n$, respectively, at different concentrations of I_3^-. The excited Ru(II) bound to the SiO_2 surface is readily quenched by I_3^-. This is evident from the decreased emission lifetime of Ru(II)* with increasing I_3^- concentration. From the dependence of the emission decay rate constant versus I_3^- concentration, we obtain a bimolecular rate constant of 1.9×10^{10} M^{-1} s^{-1}. That the rate constant is close to the value of a diffusion-controlled reaction suggests the ability of I_3^- to intercept excited Ru(II)* very effectively. To the best of our knowledge, this is the first report that directly probes the quenching between Ru(II)* and I_3^-. Ru(II)* can be quenched both reductively and oxidatively. In previous studies, we have probed the reductive quenching of Ru(II)* by I^- by adsorbing the sensitizer onto a SiO_2 surface. The bimolecular quenching for this reaction was determined to be 1×10^8 M^{-1} s^{-1}.[13] In the present investigation, the quenching of Ru(II)* by I_3^- is oxidative with a greater rate constant than that observed with iodide. The undesirable quenching by the redox couple can pose a problem if it competes with the charge injection from Ru(II)* to SnO_2 or TiO_2. When one considers the high concentration of iodide and triiodide employed in the electrolyte, such a competitive process cannot be ruled out.

Interestingly, when we deposit C_{60} clusters onto Ru(II) (Figure 5B) we do not observe an emission decay dependence on the I_3^- concentration. The emission decay traces in Figure 5B show little variation when the concentration of I_3^- in solution is increased from 0 to 0.8 mM. Depositing C_{60} clusters onto Ru(II) thus enabled us to minimize the interaction between Ru(II)* and I_3^-. This observation explains the benefit of enhancing the IPCE of SnO_2/Ru(II) and TiO_2/Ru(II) films. Although in a dye-sensitized solar cell the charge injection is expected to be fast (on the subpicosecond-to-nanosecond time scale),[8−10] the high quenching rate constant of I_3^- can be a limiting factor especially when one employs the redox couple at relatively high concentration levels.

Whereas the above experiments demonstrate the beneficial role of C_{60} clusters in minimizing the interaction between Ru(II)* and I_3^-, one needs to understand the mechanism by which it shuttles electrons and regenerates the sensitizer. As demonstrated earlier, the absorption of C_{60} clusters extends well into the IR region, and when excited in the presence of iodide, C_{60} undergoes electron transfer to generate C_{60}^- ions. The C_{60}^- ions become stabilized in the cluster and donate electrons whenever they encounters an oxidized sensitizer (viz., Ru(III)). Neither C_{60} nor C_{60}^- has any significant influence on the excited-state dynamics of Ru(II*). (A comparison of the Ru(II*) emission decay in Figure 5A and B shows no significant effect of C_{60}.) The only role of the C_{60} cluster is to shuttle the electron between Ru(III) and I_3^-. A similar mediating role of C_{60}/C_{60}^- in the electrocatalytic oxidation of ferrocene has been demonstrated in a cyclic voltammetric study.[19] Moreover, charge transport by lateral electron hopping within the fullerene monolayer is observed by depositing these clusters on an insulating oxide (ZrO_2).[20] Apparent diffusion coefficients as high as 1.5×10^{-8} cm^2 s^{-1} were measured for the electron-hopping process in this study. The energy-level diagram illustrating various charge-transfer processes that contribute to the enhancement of the photocurrent generation of the OTE/TiO_2/Ru(II)/$(C_{60})_n$ electrode is shown in Scheme 3.

Most of the visible excitation is centered around Ru(II) to induce charge injection into TiO_2 nanocrystallites. However, long-wavelength excitation can be utilized to generate triplet excited C_{60} and form C_{60}^- ions within the cluster framework. The C_{60}/C_{60}^- redox couple acts as an electron relay to regenerate the sensitizer. In the past, a similar concept of regenerating sensitizer has been attempted using a p-type semiconductor or solid electrolytes.[21−24] In most of these cases, the performance of the cell remains quite low. The present approach of using

SCHEME 3: Energy Levels[a] of Various Redox Couples Responsible for the Charge-Transfer Processes

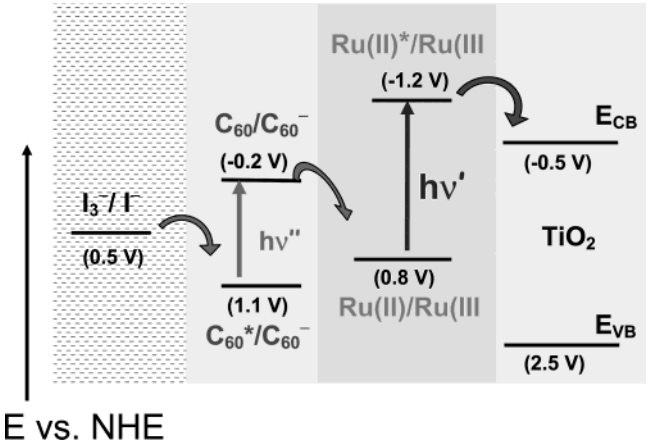

[a] Not to scale.

C_{60}/C_{60}^- as an electron shuttle could pave the way for improved photoelectrochemical cells.

Conclusions

C_{60} clusters are quite effective as electron relays and facilitate the regeneration of the sensitizer in a dye-sensitization-based photochemical solar cell. By minimizing the redox couple-induced deactivation of the excited sensitizer, it is possible to improve the efficiency of photocurrent generation in such cells.

Acknowledgment. The research described herein is supported by the Office of Basic Energy Science of the Department of Energy. This is contribution no. NDRL 4506 from the Notre Dame Radiation Laboratory. S.H. acknowledges the support of the Natural Sciences and Engineering Research Council of Canada.

References and Notes

(1) Graetzel, M. Nanocrystalline Electronic Junctions. In *Semiconductor Nanoclusters: Physical, Chemical and Catalytic Aspects.*; Kamat, P. V., Meisel, D., Eds.; Elsevier Science: Amsterdam, 1997; p 353.

(2) Graetzel, M. *Nature* **2001**, *414*, 338.

(3) Cahen, D.; Graetzel, M.; Guillemoles, J. F.; Hodes, G. Dye Sensitized Solar Cells: Principles of Operation. In *Electrochemistry of Nanomaterials*; Hodes, G., Ed.; Wiley-VCH Verlag GmbH: Weinheim, Germany, 2001; p 201.

(4) Argazzi, R.; Bignozzi, C. A.; Heimer, T. A.; Castellano, F. N.; Meyer, G. J. *Inorg. Chem.* **1994**, *33*, 5741.

(5) Dressick, W. J.; Meyer, T. J.; Durham, B.; Rillema, D. P. *Inorg. Chem.* **1982**, *21*, 3451.

(6) Duffy, N. W.; Peter, L. M.; Rajapakse, R. M. G.; Wijayantha, K. J. U. *J. Phys. Chem. B* **2000**, *104*, 8916.

(7) Heimer, T. A.; Heilweil, E. J.; Bignozzi, C. A.; Meyer, G. J. *J. Phys. Chem. A* **2000**, *104*, 4256.

(8) Fessenden, R. W.; Kamat, P. V. *J. Phys. Chem.* **1995**, *99*, 12902.

(9) Ramakrishna, S.; Willig, F. *J. Phys. Chem. B* **2000**, *104*, 68.

(10) Asbury, J. B.; Randy, J.; Ellingson, R. J.; Ghosh, H. N.; Ferrere, S.; Nozik, A. J.; Lian, T. *J. Phys. Chem. B* **1999**, *103*, 3110.

(11) Thompson, D. W.; Kelly, C. A.; Farzad, F.; Meyer, G. J. *Langmuir* **1999**, *15*, 650.

(12) Bergeron, B. V.; Meyer, G. J. *J. Phys. Chem. B* **2003**, *107*, 245.

(13) Nasr, C.; Hotchandani, S.; Kamat, P. V. *J. Phys. Chem. B* **1998**, *102*, 4944.

(14) Bedja, I.; Hotchandani, S.; Kamat, P. V. *J. Phys. Chem.* **1994**, *98*, 4133.

(15) Subramanian, V.; Wolf, E.; Kamat, P. V. *J. Phys. Chem. B* **2001**, *105*, 11439.

(16) Kamat, P. V.; Barazzouk, S.; George Thomas, K.; Hotchandani, S. *J. Phys. Chem. B* **2000**, *104*, 4014.

(17) Kamat, P. V.; Barazzouk, S.; Hotchandani, S. *Adv. Mater.* **2001**, *13*, 1614.

(18) Thomas, K. G.; Biju, V.; George, M. V.; Guldi, D. M.; Kamat, P. V. *J. Phys. Chem. B* **1999**, *103*, 8864.

(19) Barazzouk, S.; Hotchandani, S.; Kamat, P. V. *J. Mater. Chem.* **2002**, *12*, 2021.

(20) Papageorgiou, N.; Grätzel, M.; Enger, O.; Bonifazi, D.; Diederich, F. *J. Phys. Chem. B* **2002**, *106*, 3813.

(21) Nogueira, A. F.; De Paoli, M.-A.; Ivan Montanari, I.; Richard Monkhouse, R.; Jenny Nelson, J.; Durrant, J. R. *J. Phys. Chem. B* **2001**, *105*, 7517.

(22) Meng, Q.-B.; Takahashi, K.; Zhang, X.-T.; Sutanto, I.; Rao, T. N.; Sato, O.; Fujishima, A.; Watanabe, H.; Nakamori, T.; Uragami, M. *Langmuir* **2003**, *19*, 3572.

(23) Perera, V. P. S.; Pitigala, P. K. D. D. P.; Jayaweera, P. V. V.; Bandaranayake, K. M. P.; Tennakone, K. *J. Phys. Chem. B* **2003**, *107*, 13758.

(24) Wang, P.; Zakeeruddin, S. M.; Moser, J.-E.; Gratzel, M. *J. Phys. Chem. B* **2003**, *107*, 13280.